

2. ISEE International Joint Research Program 目次詳細

(所属・職名は2021年3月現在)
(Affiliation and Department displayed are current as of March 2021.)

(注1) : 新型コロナウイルスの影響で2021年度に延期し実施
(注2) : 新型コロナウイルスの影響で中止

研究代表者 Principal Investigator	所属機関 Affiliation	所属部局 Department	職名 Position	研究課題名 Project Title	頁 Page	備考 Remarks
Rangaiah Kariyappa	Indian Institute of Astrophysics	Department of Science & Technology, Solar & Space Physics Division	Former Professor	Understand the EUV and UV (PROBA2/LYRA) and X-ray(GOES 1-8 A) irradiance variability from spatially resolved images of SDO/AIA/HMI & PROBA2/SWAP and Hinode/XRT instruments	57	(注2)
Chen Xingyao	National Astronomical Observatories of Chinese Academy of Sciences	Key Laboratory of Solar Activity	Research Assistant	Quasi-periodic Pulsations from solar radio and microwave observations	58	(注2)
Abadi Prayitno	Indonesian National Research and Innovation Agency (BRIN)	Research Center for Climate and Atmosphere	Researcher	Empirical Model of Equatorial Plasma Bubble Occurrence Rate in Southeast Asia deduced from GPS Receivers	59	(注1)
Xia Yuan	Nanjing Xiaozhuang University	School of Electronic Engineering	Lecturer	Winter sudden stratospheric warming (SSW) impact on mesosphere sodium layer observed at middle and high latitudes	61	(注1)
Opgenoorth Hermann	University of Umea	Physics	Professor Emeritus	Study of sub-auroral storm time magnetic and convection disturbances	63	(注2)
PORUNAKATU RADHAKRISHNA SHREEDEVI	Beihang University	Beihang University	Postdoctoral Researcher	Understanding the role of EMIC wave scattering in causing ion precipitation into the ionosphere: Comparison of SWMF simulations with Arase and PWING observations	64	(注1)
Lazzara Matthew	University of Wisconsin-Madison	University of Wisconsin-Madison, Space Science and Engineering Center	Senior Scientist	Creation of a new high-quality dataset of East Antarctic meteorological observations	66	(注1)
Gordovskyy Mykola	University of Manchester	Physics and Astronomy	Research Associate	Fluid-kinetic modelling of magnetic reconnection in solar flares and solar energetic particle escape into the heliosphere	68	(注1)
Braga Carlos Roberto	George Mason University	Department of Physics and Astronomy	Senior Research Scientist	Predicting coronal mass ejections Time-of-arrival and magnetic field orientation in the Earth's vicinity using observations and MHD propagation	70	(注2)
AZIZI HajiHosseini	University of Kurdistan	Department of Mining, Faculty of Engineering	Professor	Beryllium-10 (¹⁰ Be)-Nd isotope analysis to investigate magma source of the Quaternary volcanoes in northwest Iran	71	(注1)
Min Kyungguk	Chungnam National University	Department of Astronomy and Space Science	Assistant Professor	Understanding the Generation Process of Fast Magnetosonic Waves by Combining ERG Observations and PIC Simulations	73	(注2)
JIE REN	Peking University	Institute of Space Physics and Applied Technology	Assistant Researcher	ULF Waves' Interaction with the Charged Particles and the Effects on the Whistler Mode Waves	74	(注2)

研究代表者 Principal Investigator	所属機関 Affiliation	所属部局 Department	職名 Position	研究課題名 Project Title	頁 Page	備考 Remarks
CHEN LINJIE	National Astronomical Observatories, Chinese Academy of Sciences	Solar Physics Division / Mingantu Observation Station	Associate Researcher/Professor	Studying the solar wind with the multi-station Interplanetary Scintillation (IPS) Telescope	75	(注2)
Krucker Samuel	FHNW	Institute for Data Science	Professor	The NoRH/RHESSI flare catalogue: time-dependent analysis	76	(注2)
Mouikis Christoforos	University of New Hampshire	Space Science Center	Research Scientist	The impact of storm-time ion composition changes in the near-earth plasma sheet on the ring current pressure development	77	(注2)
Prof. Dr. Ulrike Langematz	Freie Universität Berlin	Institute of Meteorology	Professor	Modeling the transport and deposition of cosmogenic isotopes of historical MIYAKE Events and recent decades.	78	(注1)

(Form 2-2)

**Understand the EUV and UV (PROBA2/LYRA) and X-ray(GOES 1-8
A) irradiance variability from spatially resolved images of
SDO/AIA/HMI & PROBA2/SWAP and Hinode/XRT instruments**

Rangaiah Kariyappa
Indian Institute of Astrophysics
Department of Science & Technology, Solar & Space Physics Division

Cancelled due to COVID-19

(Form 2-2)

Quasi-periodic Pulsations from solar radio and microwave observations

Chen Xingyao

National Astronomical Observatories of Chinese Academy of Sciences

Key Laboratory of Solar Activity

Cancelled due to COVID-19

(Form 2-2)

Empirical Model of Equatorial Plasma Bubble Occurrence Rate in Southeast Asia deduced from GPS Receivers

Prayitno Abadi (Space Research Center, Indonesian National Agency of Research and Innovation (BRIN))

1. Purpose

The ionospheric irregularities (plasma density fluctuation) embedded in the phenomenon so-called equatorial plasma bubble (EPB) have disadvantageous effects on trans-ionospheric radio wave propagation used in modern communications and navigation systems. This problem calls for a simple but robust model to predict the EPB occurrence. The day-to-day variability in EPB occurrence remains challenging, but scientists have attempted to investigate the factors that control the generation of EPB. Hence, the development of an empirical model of EPB could be necessary in space weather services. This study aims to develop an empirical model of EPB deduced from the ground observations in Southeast Asia.

2. Methods

The observations used in this study are an ionosonde installed in equatorial region and a GPS receiver in low-latitude region. The ionosonde is located at Chumphon (CPN, 99.4°E, 10.7°N, mag. lat.: 1.3°N) in Thailand. The GPS receiver is sited at Kototabang (KTB, 100.3°E, 0.20°S, mag. lat.: 9.5°S) in Indonesia. In this study, the empirical model of EPB is defined as a statistical model to connects the controlling factors of EPB occurrence to the probability of EPB occurrence. From the previous literature, the controlling factors of EPB occurrence are evening upward plasma drift in the evening equatorial region (hereafter denoted as v), solar activity parameterized by solar flux $F_{10.7}$, and geomagnetic activity measured by Kp index. The observation of v is derived from the time derivative of virtual height ($h'F$) at 3 MHz around sunset observed by CPN ionosonde. The occurrences of EPBs can be identified by the amplitude scintillation occurrences from the observation of GPS receiver at KTB. The logistic regression is implemented to build a model of the EPB occurrence probability, and it can be expressed by

$$y = \frac{1}{1 + \exp(-z)} \quad (1)$$

$$z = \beta_0 + \beta_1 v + \beta_2 F_{10.7} + \beta_3 Kp \quad (2)$$

where y is the logistic regression that represents the probability of EPB occurrence, z is a linear function consisting of v , $F_{10.7}$, and Kp , and β_j (j from 0 to 3) are regression coefficients. Parameters

of v , $F_{10.7}$ and Kp in the z -function (Eq. (2)) are defined as predictors for plasma bubble occurrence. The dataset of this study contains 427 data points where each data point consists of v , $F_{10.7}$, Kp , and the EPB occurrence. The dataset is collected from the observations during equinox seasons (March–April and September–October) from 2003 to 2016. 70% of dataset is used for training set to derive β_j for the z -function (Eq. (2)), and the remaining 30% of dataset is used to test the performance of the z -function in forecasting the EPB occurrence. In the training set, β_j can be solved by the gradient descent technique.

3. Results

In training set, the expression $z = -2.58 + 0.15v + 0.01F_{10.7} - 0.46Kp$ is obtained. This z -function is then implemented in logistic regression (Eq. (1)) to classify night with and without the EPB occurrence, and $y \geq 0.5$ and $y < 0.5$ can represent the occurrence and non-occurrence of EPB, respectively, with an accuracy of 0.8 and a true skill score (TSS) of 0.6. Similarly, this z -function implemented in the logistic regression can classify nights with and without EPB occurrence in the testing dataset with an accuracy of 0.8 and a TSS of 0.6. In conclusion, the z -function and the y values of the proposed model could be a simple but robust mathematical model for daily nowcasting the occurrence or non-occurrence of EPBs when new inputs of v , $F_{10.7}$ and Kp are added.

4. Period of Stay in ISEE

Not applicable due to travel restriction during the COVID-19 pandemic.

5. List of Publication

Abadi, P.; Ahmad, U. A.; Otsuka, Y.; Jamjareegulgarn, P.; Martiningrum, D. R.; Faturahman, A.; S. Perwitasari; Saputra, R. E.; Septiawan, R. R. Modeling post-sunset ESF occurrence as functions of evening upward plasma drift, solar activity, and geomagnetic activity using logistic regression. Remote Sens. (under revision).

6. Future works

The mathematical model of the EPB occurrence found in this study requires real-time observation of v if it is implemented in space weather services. This work must be complemented by the automatic calculation of v from the ionosonde. Future work needs to develop an automatic scaling of $h'F$ from the ionosonde in the evening sector of the equatorial region. In addition, the mathematical model found in this study should be validated using data observation in solstice months to determine the consistency and accuracy of the model performance.

Winter sudden stratospheric warming (SSW) impact on mesosphere sodium layer observed at middle and high latitudes

Yuan Xia

NanJing Xiaozhuang University

Nanjing, 211171, China

Summary:

Metallic sodium (Na) layer in the mesosphere and lower thermosphere (MLT) region is good tracer for studying atmospheric dynamics and photochemistry. It has been known that sudden stratosphere warming events (SSWs) have impacts not only at high latitudes but also at mid-latitudes and even equatorial latitudes.

Based on the Na lidar observations and TIMED/SABER (Sounding of Atmosphere by Broadband Emission radiometry on board Thermosphere-Ionosphere-Mesosphere Energetics and Coupling) satellite observations, we investigated a Na layer bottom enhancement event observed at middle latitude (40.41°N, 116.01°E). The significant Na density increase near 75 km was found to be accompanied by cooling anomaly in the stratosphere and warming anomaly in the mesosphere, which are exactly the opposite of the temperature anomalies observed during SSW event. It is noted that indeed a minor SSW occurred around January 4, 2015, about two weeks before the Na layer bottom enhancement event (December 17, 2014). The variations of planetary waves (PWs) in geopotential height in mid-December, 2014 are consistent with the general results prior to a SSW. These results hint an association of the observed atmospheric anomalies with SSW. The warming anomaly in the upper mesosphere contributed to the liberation of Na atoms from its reservoir (e.g., NaHCO₃) near the Na layer bottom via neutral chemical reactions, whose rate are proportional to temperature. Sudden enhancement of PWs and their interactions with the mean flow are widely accepted as the cause of SSWs. The lidar measurements of the Na layer, zonal wind results from a nearby meteor radar, global satellite observations as well as reanalysis data reveal the close correlation between the variation of Na layer bottom and planetary scale atmospheric disturbances, as evidenced by the eastward transportation structures seen in the temporal-longitudinal variations of background atmospheric parameters in both mesopause and stratosphere. We finished a paper and submitted to ACP under review. The initial analysis of Na lidar data in Tromsø (69.6°N, 19.2°E) showed Na density increase below 85 km and decrease above 90 km after January 7, 2015. This is also likely linked to the minor SSW occurred around January 4, 2015.

The study on the impact of SSW on the Na layer at middle and high latitudes will be

continued by including more Na layer observational data in both Tromsø and Beijing.

Period of stay:

Due to the novel coronavirus epidemic, the visit and stay in ISEE was postponed and finally cancelled. The PI worked with the ISEE collaborator through on-line meeting and emails and benefited much from discussion with Prof.Nozawa.

List of publications:

- (1) Yuan Xia, Satonori Nozawa, Jing Jiao, Jihong Wang, Faquan Li, Xuewu Cheng, Yong Yang, Lifang Du, Guotao Yang: Statistical study on sporadic sodium layers (SSLs) based on diurnal sodium lidar observations at Beijing, China (40.5 °N, 116 °E), *Journal of Atmospheric and Solar-Terrestrial Physics*, 212: 105512, 2021.
- (2) Xia, Y., Jiao, J., Nozawa, S., Cheng, X., Wang, J., Du, L., Li, Y., Zheng, H., Li, F., and Yang, G.: Significant enhancements of the mesospheric Na layer bottom below 75 km observed by a full-diurnal-cycle lidar at Beijing (40.41 °N, 116.01 °E), China, *Atmos. Chem. Phys. Discuss.* [preprint], <https://doi.org/10.5194/acp-2022-112>, in review, 2022.

(Form 2-2)

Study of sub-auroral storm time magnetic and convection disturbances

Opgenoorth Hermann
University of Umea
Physics

Cancelled due to COVID-19

Understanding the role of EMIC wave scattering in causing ion precipitation into the ionosphere: Comparison of SWMF simulations with Arase and PWING observations

Shreedevi P R,

School of Space and Environment, Beihang University, Beijing, China,

Purpose: It is known that magnetospheric wave activity drives the ion precipitation which can become an important source of energy flux into the ionosphere and strongly affect the dynamics of the magnetosphere-ionosphere coupling during geomagnetic storms. However, the contribution of ions is usually neglected as electron precipitation is believed to be the major source of energy into the ionosphere. To obtain accurate predictions of the storm-time ionospheric dynamics, it is very important to account for the contributions from ions also. The main purpose of the proposed study is to understand the processes responsible for the spatial and temporal evolution of localized ion precipitation during geomagnetic storms. The two main objectives of the study are: (1) to identify and confirm the causative mechanisms responsible for the spatial and temporal evolution of localized ion precipitation in the sub-auroral latitudes, and (2) to assess the performance of the BATSRUS+RAM SCBE model in reproducing the realistic ion precipitation into the ionosphere.

Methods: We chose the intense geomagnetic storm event of 27-28 May 2017 for the case study. A combination of physics based models (BATSRUS+RAM-SCBE) and ground/satellite based observations were used to understand the temporal and spatial evolution of the proton precipitation into the ionosphere and its correspondence to the Electro Magnetic Ion Cyclotron (EMIC) wave activity in the inner magnetosphere during the geomagnetic storm event. We first examined the particle measurements from DMSP satellites to understand the response of the topside mid-latitude ionosphere to the storm event. Dynamic spectra of magnetic field as measured by the Van Allen Probes satellite were used to confirm the intensity and location of EMIC wave activity in the inner magnetosphere during the storm. Ground magnetic field measurements from high latitude stations were used to understand the evolution of EMIC waves at sub-auroral latitudes. We compared the simulated ion fluxes obtained from the BATSRUS+RAM SCBE model simulations with and without EMIC wave particle interactions to study the role of EMIC wave-particle interaction in causing ion precipitation into the ionosphere.

Results: During the geomagnetic storm of 27-28 May 2017, the Van Allen Probes satellite

observed typical signatures of EMIC waves in the inner magnetosphere i.e., at 4 to 6 Re in the evening sector. Ground magnetometers at high latitude stations also showed the presence of PC1/EMIC waves after 1600 UT on 27 May 2017. During the main phase of the storm, the DMSP satellites observed enhanced proton precipitation at locations where the ground/space based magnetic field measurements showed the presence of enhanced EMIC wave activity. There is little or no electron precipitation at these regions. Or in other words, these regions are dominated by ion precipitation. Using the SWMF (BATSRUS + RAM SCBE), we conducted two simulations to study the ion precipitation, i.e., without EMIC waves and with EMIC waves. We studied the global distribution of precipitating proton fluxes obtained from the simulations. We noted that in the absence of EMIC wave scattering, the precipitating proton fluxes are mostly observed in the midnight sector with maximum fluxes at L=5-6 Re. In the presence of EMIC waves, there is additional precipitation in the noon-midnight sector, with maximum around L=4-5 Re. The new proton fluxes are about an order of magnitude higher than that seen in the case without EMIC waves. This shows that EMIC wave scattering can cause enhancements in the precipitating proton fluxes. We then compared the energy fluxes obtained from the simulations with the DMSP observations at regions where the RBSP measurements show the presence of EMIC wave activity. In the case of simulations without including EMIC waves, the ion energy fluxes were very weak and the integrated proton energy flux do not agree with the DMSP observations. However, the simulations with EMIC waves captured reasonably well the <30 keV ion fluxes at sub auroral latitudes. The integrated ion energy flux obtained from the simulation with EMIC waves was also comparable with the DMSP observations. The model however does not capture the equatorward edge of the ion precipitation well, which needs to be improved. We conclude that EMIC wave scattering is a causative mechanism for the enhanced precipitation of ions at subauroral regions during the 27-28 May 2017 storm. And the RAM-SCBE model is able to capture reasonably well the precipitation of <30 keV proton fluxes at DMSP altitudes. We are continuing this work to conduct further analysis of several ionospheric datasets from conjugate locations which is necessary to obtain a more comprehensive understanding of the role of EMIC waves in the spatio-temporal evolution of the ion precipitation and its impact on the mid latitude ionospheric dynamics.

Periods of stay in ISEE: The PI was unable to visit ISEE due to travel restrictions imposed by the COVID 19 pandemic

List of Publications: None

(Form 2-2)

Creation of a new high-quality dataset of East Antarctic meteorological observations

Principal Investigator: Matthew A. Lazzara (University of Wisconsin-Madison)

This study was carried out in collaboration with David Mikolajczyk (University of Wisconsin-Madison), Shohei Morino (Nagoya University), and Naoyuki Kurita (Nagoya University). Oversea travel has been restricted due to the COVID-19 pandemic. As a result, we gave up on the proposed travel plan and pursued a part of the project. Here we report the summary of our study conducted in this fiscal year.

Motivation:

Near-surface air temperature measurements over the Antarctic Plateau (AP) are important both for climate change monitoring and for model validation. On the inland AP, automatic weather stations (AWSs) are installed and transmit observed temperature data via satellite. It is, however, difficult to obtain accurate temperatures on the snow-covered regions as most temperature measurements are subject to systematic errors resulting from the heating of the sensor by solar radiation. To minimize these errors, an AWS temperature sensor is enclosed in a radiation shield with a forced ventilation (FV) system. Due to the limited power at AWS sites to run ventilated shields, naturally ventilated (NV) radiation shields are primarily used in Antarctica instead of FV radiation shields. The NV can only reduce the influence of radiative heating and cannot completely eliminate the errors. When ventilation is inadequate to remove the influence of radiative heating, NV temperature measurements result in higher temperature values (hereafter referred to as radiative error) than the FV measurements. Through this project, we examined radiative errors of NV temperature measurement in inland AP and explored the correction method of these errors.

Methodology:

Recently, the Japanese Antarctic Research Expedition (JARE) deployed the latest version AWSs in inland Dronning Maud Land (DML) in the East Antarctica. In 2018, the JARE installed AWS at two sites, NDF (77.79°S, 39.06°E, 3742 m a.s.l.) in January and Relay Station (74.01°S, 42.98°E, 3354 m a.s.l.) in October. These AWSs measure air temperature by the FV system. In addition to the newly installed AWSs by JARE (JARE-AWSs), there are four AWSs (Mizuho, Relay Station, JASE2007 and Dome Fuji) deployed by the University of Wisconsin's Antarctic

Meteorological Research and Data Center (AMRDC; the AWS referred to here after as UW-AWSs). These AWSs use a NV shield for air temperature measurement. In this study, we examined and quantified the radiative errors through the comparison between the JARE-AWSs at NDF and Relay Station and the UW-AWSs at Relay Station and Dome Fuji.

Results:

Similar to the past studies, air temperatures measured by a NV shield in inland DML showed higher values than those by a FV shield due to solar radiative heating. In austral summer, the temperature bias between the FV sensor and the NV sensor never reached zero due to continuous sunlight. The hourly mean temperature errors reached up to 8°C at noon on a sunny day with weak wind conditions. Radiative errors were strong functions of reflected solar radiation and wind speed. The errors increased linearly with increasing reflected shortwave radiation and decreased non-linearly with increasing wind speed. These features are consistent with previous related studies. To quantify the radiative errors, we applied an existing correction model based on a regression approach. We found that this approach successfully reduced both the mean and root-mean-square error (RMSE) of the radiative error after the correction. At Relay Station, the reduction of RMSE for the errors of the UW-AWS reached more than 70%. The robustness of the correction model indicates that we can use the corrected temperature data instead of a quality control method to remove radiative errors during weak wind conditions. The UW-AWSs were installed in the mid-1990s in inland DML and have since observed air temperature and wind speed at Mizuho, Relay Station, JASE2007 and Dome Fuji. The fact that the radiative error depends on the shape and design of the radiation shield suggests that the regression line of Relay Station could apply to the other AWSs since these are equipped with the same radiation shield. Thus, reducing the radiative errors can increase the validity of temperature data in inland DML on the East Antarctic Plateau.

List of publication:

Morino, S., N.Kurita, N.Hirasawa, H.Motoyama, K.Sugiura, M.A.Lazzara, D.Mikolajczyk, L.Welhouse, L.Keller, and G. Weidner: Comparison of ventilated and unventilated air temperature measurements in inland Dronning Maud Land on the East Antarctic Plateau, *J. Atmos. Oceanic technol.*, 38, 2061-2070, <https://doi.org/10.1175/JTECH-D-21-0107.1>, 2021.

Fluid-kinetic modelling of magnetic reconnection in solar flares and their impact on the heliosphere

PI: Mykola Gordovskyy (University of Manchester)

Background:

High-energy particles carry a substantial amount of energy released in solar flares. Furthermore, energetic electrons and ions escaping from the solar corona into the heliosphere are an important factor affecting the space weather. The aim of this collaborative research is to study energetic particle escape into the heliosphere during solar flares. The main objective for the 2021-22 project was to model particle acceleration in solar flares, and investigate compare their properties in the corona and in the inner heliosphere.

Outcomes of the project:

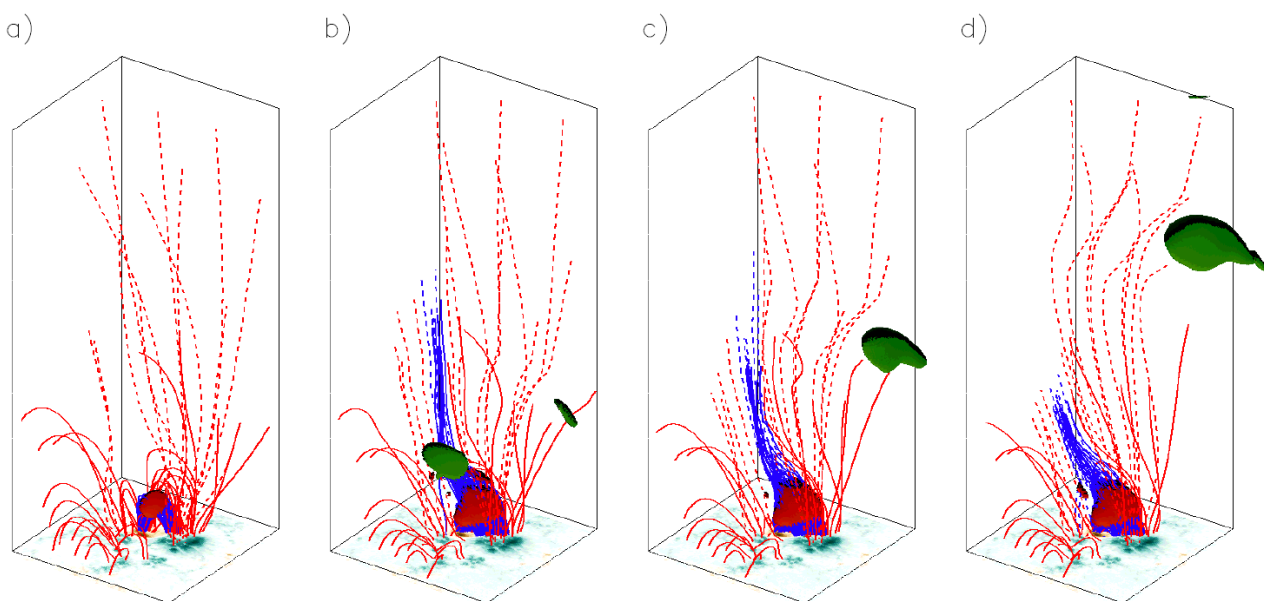


Figure 1: Snapshots of the magnetohydrodynamic model of an X-class flare observed on the 6th of September 2011. Blue and red lines show magnetic field, red-brown surfaces show energy release/particle acceleration regions. Green surfaces denote volumes of plasma moving at high speed.

The collaborative research between the solar group in the University of Manchester and ISEE, University of Nagoya has begun in 2019. The main outcome of the first year was the first ever magnetohydrodynamic-particle model of an actual solar flare, which has managed to successfully predict observables, such as locations and relative intensities of hard X-ray emission sources produced by precipitating energetic electrons. Building on that approach, in 2020-21, we have constructed magnetohydrodynamic-particle models of two solar flares (X-class flare observed on 6 September 2011 and M-class flare observed on 19 June 2013) with the magnetic flux partially open to the heliosphere, resulting in a significant number of energetic particles escaping from the solar corona into the heliosphere (Figure 1). Good agreement between the observational features shown by these flares and synthetic observables derived using the computational models of these flares (e.g. locations and relative intensities of HXR sources, large-scale motions of plasma visible in extreme UV) indicated that the developed models are adequate and, hence, can be used to study the dynamics of energetic particles in these events.

Based on the developed computational models, we show that the energy spectra of energetic particles precipitating in the corona and ejected towards the heliosphere are different. Thus, the power-law spectral indices δ of the escaping populations of electrons and protons appear to be approximately 0.5 units higher (i.e. their energy spectra are softer) compared to their precipitating counterparts. (Here, the energy spectra are fitted by the power-law distributions $N(E) \sim E^{-\delta}$). We also find that the number of escaping energetic particles is significantly lower than the number of precipitating particles; the ratio of escaping to precipitating electrons in both considered flares peaks at 20-25%. This ratio changes with time, depending on the dynamics of magnetic field in the flare.

Therefore, our study shows that energetic particle populations originating from the same acceleration region of the same flaring event will have different energy spectra, and may have different temporal evolution (i.e. show different variations of energetic particle flux as a function of time) in the corona and the heliosphere. This is an important finding: it shows that the observed difference between the properties of energetic particle populations in the corona and near the Earth can be explained by the intrinsic properties of the acceleration region alone.

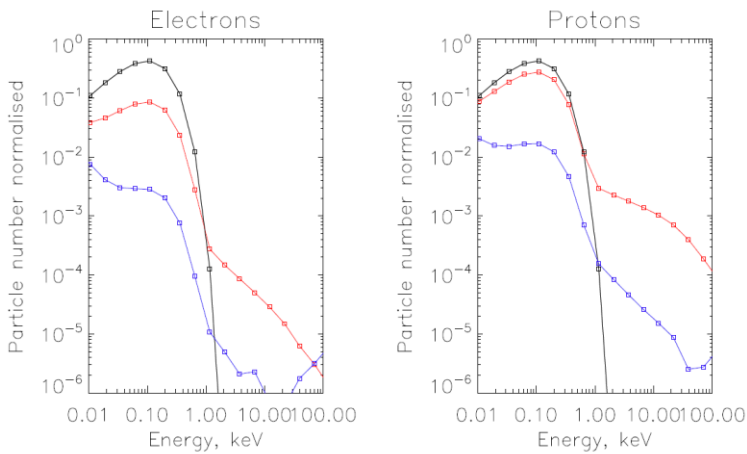


Figure 2: Energy spectra of electrons and protons accelerated in the considered solar flare (06/09/2011 event), and precipitating in the solar corona (red lines) and escaping into the heliosphere (blue lines). Black lines denote initial thermal spectra.

Although, the travel between the UK and Japan was restricted during 2020-2021 due to ongoing Covid-19 pandemics and we were unable to travel to ISEE, Nagoya, we had a number of remote discussion meetings, from which this collaborative research strongly benefited. At present, we are preparing for publication a manuscript based on the above results. It is expected to be submitted by the end of April 2022.

Future plans:

Overall, this joint research was extremely useful. We plan to continue it; the objective for the next 6 months will be to identify solar flares with particle emission observed in situ either by Parker Solar Probe or Solar Orbiter mission, and apply the developed approach to modelling these events.

(Form 2-2)

Predicting coronal mass ejections Time-of-arrival and magnetic field orientation in the Earth's vicinity using observations and MHD propagation

Braga Carlos Roberto
George Mason University
Department of Physics and Astronomy

Cancelled due to COVID-19

Project Title: Beryllium-10 (^{10}Be)-Nd isotope analysis to investigate magma source of the Quaternary volcanoes in northwest Iran

HajiHossein AZIZI
Professor
University of Kurdistan, Iran

This research work was carried out in collaboration with Masayo Minami (ISEE/Nagoya University), Yoshihiro Asahara (Graduate School of Environmental Studies/Nagoya University), and Motohiro Tsuboi (School of Biological and Environmental Sciences/Kwansei Gakuin University).

Purpose

Constraining of the magma sources in NW Iran based on the short-lived radioactive isotope of ^{10}Be , and combination with ^{87}Sr , ^{143}Nd , and ^{176}Hf derived from long-lived radioactive isotopes of ^{87}Rb , ^{147}Sm , and ^{176}Lu .

Methods

1. Sampling for the young (Neogene to Quaternary period) magmatic rocks in northwest Iran.
2. Chemical separation of Be from the samples based on calibration result of the cation and anion exchange resin columns at ISEE.
3. Measurement of ^{10}Be with Tandetron AMS.
4. Radiometric dating of zircon grains in the young rocks by LA-ICPMS.
5. Quantitative analysis of Li, Be, and their related elements by XRF and ICP-MS.
6. Sr-Nd isotope analysis using TIMS.
7. Hf isotope analysis using MC-ICP-MS.

Results

This research started from fieldwork to collect samples of the different types of young volcanic rocks in NW Iran in 2020. At first, we focused on the chemical and Sr-Nd-Hf isotopic data to clarify the primary tectonic setting of these rocks. Based on our previous findings, we reported the Miocene post-collision andesite for the first time in NW Iran, and the occurrence of the Miocene post-collision andesite is a rare case in the world (Azizi et al., 2021). Our previous and new data for whole-rock chemistry including Li concentrations with zircon U–Pb ages of 18 to 15 Ma show that most of the Early Miocene magmatic rocks are andesite with subordinate dacite. The magmatic rocks have low contents of Mg, Ni, Cr, Ti, Nb, and Ta, and high concentrations of Li, large ion lithophile elements such as K, Rb, and Ba, and light rare earth elements. These geochemical features support the idea that the Early Miocene andesites in NW Iran were generated after the collision and were associated with doubling of the thickness of the continental crust in the Zagros suture zone, thinning of continental crust far from the Zagros suture zone, and development of shallow-basin sedimentary rocks in NW Iran. Partial melting of mafic calc-alkaline bodies at depth or highly metasomatized fossil mantle owing to thinning of continental crust and asthenospheric upwelling may be possible sources for the Miocene

andesite. We conclude that the andesitic rocks, even with typical arc signatures, were not always generated in an active margin regime and that some were probably generated in a post-collision tectonic regime.

Most of our works have focused on heavy isotopes (Sr-Nd-Hf) with chemical compositions including some light elements such as Li to constrain tectonic setting, and however we have not had direct evidence on the contribution of young subducted sediment to the magma source yet. The result of the ^{10}Be contents is very important to reveal the recycling of the "atmospheric" isotope in the subduction zone and post-collision system. During my staying period at ISEE, we set up both cation and anion exchange resin columns in the chemistry laboratory of the Chronological Research Division at ISEE and then made chemical separations of Be from the 40 rock samples, chemical and Sr-Nd-Hf isotopic data for which has already been obtained at Nagoya University and the University of Ryukyus.

The samples are now ready for ^{10}Be measurements by AMS, and ^{10}Be data will appear in a few months. We will add chemical and Sr-Nd-Hf isotopic data including Li and Be for some more samples during my next staying at ISEE this autumn (2022), and hope to publish these results in some high-quality journals shortly.

Period of stay in ISEE

My period of stay at Nagoya University was from 23 November 2021 to 11 February 2022.

This project was supported by ISEE/Nagoya University under ISEE International Joint Research Program and by JSPS Research Fellowship in Japan.

List of publication

Azizi, H., Daneshvar, N., Mohammadi, A., Asahara, Y., Whattam, S.A., Tsuboi, M. and Minami, M., 2021. Early Miocene post-collision andesite in the Takab area, NW Iran. *Journal of Petrology*, 62(7), p.egab022.

(Form 2-2)

**Understanding the Generation Process of Fast Magnetosonic Waves by
Combining ERG Observations and PIC Simulations**

Min Kyungguk
Chungnam National University
Department of Astronomy and Space Science

Cancelled due to COVID-19

(Form 2-2)

**ULF Waves' Interaction with the Charged Particles and the Effects on
the Whistler Mode Waves**

JIE REN

Peking University

Institute of Space Physics and Applied Technology

Cancelled due to COVID-19

(Form 2-2)

**Studying the solar wind with the multi-station Interplanetary
Scintillation (IPS) Telescope**

CHEN LINJIE

National Astronomical Observatories, Chinese Academy of Sciences
Solar Physics Division / Mingantu Observation Station

Cancelled due to COVID-19

(Form 2-2)

The NoRH/RHESSI flare catalogue: time-dependent analysis

Krucker Samuel
FHNW
Institute for Data Science

Cancelled due to COVID-19

(Form 2-2)

**The impact of storm-time ion composition changes in the near-earth
plasma sheet on the ring current pressure development**

Mouikis Christoforos
University of New Hampshire
Space Science Center

Cancelled due to COVID-19

(Form 2-2)

Modeling the transport and deposition of cosmogenic isotopes of historical MIYAKE Events and recent decades

Ulrike Langematz (Freie Universität Berlin)

Due to the covid-19 restriction, an on-site meeting in Japan could not be held. Instead, an online meeting was jointly carried out with an ISEE International Joint Research Program “Using cosmogenic isotopes to trace back large-scale atmospheric dynamics of the neutron monitor era (PI: T. Spiegl)”.